Implementation of Plastic Thickness Strain in an Equivalent Drawbead Model based on a Penalty Constraint Method.

T. Meinders, H.J.M. Geijselaers, J. Huétink
University of Twente, Faculty of Mechanical Engineering, P.O. Box 217, 7500 AE Enschede, The Netherlands

ABSTRACT: Drawbeads are applied in the deep drawing process to improve the control of the material flow during the forming operation. These drawbeads can be replaced by an equivalent drawbead in simulations of the deep drawing process. In this paper the implementation of an equivalent drawbead model in a finite element code is described. This equivalent drawbead takes not only the drawbead restraining force into account, but also the plastic thickness strain and the drawbead lift force. Simulations of the deep drawing of a rectangular product are performed to test the equivalent drawbead performance. For verification, the product is stamped as well to obtain experimental information. It can be concluded that the simulations, including the new equivalent drawbead model, show a very good correlation with the experimental results when an elastic plastic material model is used.

1. INTRODUCTION

In the deep drawing process a sheet, the 'blank', is clamped between a die and a blankholder. The specific shape of the punch and die is transferred to the sheet during the forming operation. A principle outline of this process is given in figure 1.

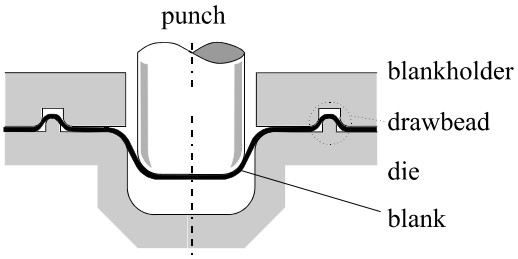

Figure 1. Deep drawing scheme including drawbeads

In practice, the material flow during deep drawing can hardly be controlled by the blankholder. To improve the material flow control, drawbeads can be used which are protrusions appearing on the die surface. Because of these drawbeads the material flow is more restrained causing a change of the strain distribution with consequently thinning of the sheet [1], [2].

Modeling the drawbead geometry accurately in a finite element program requires a large number of elements due to the small radii of the drawbead, yielding an unacceptable CPU-time. A replacement of the real drawbead by an equivalent drawbead is therefore commonly adapted in finite element codes to overcome the problem of excessive CPU-time.

Most equivalent drawbead models represent the drawbead as an additional and constant drawbead restraining force [3], [4] although this force depends on the process-progress. The changes in the strain distribution and the thinning of the blank are not taken into account in these equivalent drawbead models, which results in inaccurate simulation results.

This paper presents a new equivalent drawbead model which does incorporate the effects of sheet thinning and strain changes as well. The drawbead restraining force (D.B.R.F.), the drawbead lift force and the plastic thickness strain are considered to be history dependent.

The values of the drawbead forces and plastic thickness strain which serve as input parameters for the equivalent drawbead model can be obtained from experiments or from a 2D plane strain drawbead simulation, in which the real drawbead was accurately simulated.

The 2D drawbead model is briefly discussed in the first part of this paper. The implementation of the D.B.R.F., the lift force and the plastic thickness strain in the equivalent drawbead model are discussed in the second part of this paper. In the last part of the paper the correlation between the simulation results and the experimental results are presented.

2. 2D PLANE STRAIN DRAWBEAD MODEL

A 2D plane strain drawbead model is developed to obtain accurate data concerning the drawbead forces and thickness strain during the forming process. The 2D model uses the Arbitrary Lagrangian Eulerian formulation, available in the finite element code DiekA [5]. The sheet is modeled with four node bi-linear plane strain elements. Contact between the sheet and the tools is described with special contact elements [6]. A finite element mesh of a specific 2D drawbead model is given in Figure 2.

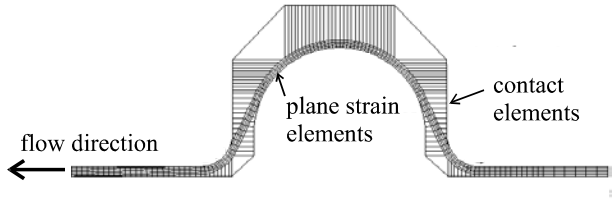

Figure 2. Finite element mesh of a 2D drawbead model

The history dependent D.B.R.F., lift force and plastic thickness strain of a drawbead are generated with this 2D drawbead model.

At Koninklijke Hoogovens N.V. an experimental setup was build to validate the performance of the numerical model. The good agreement between the experimentally data and numerical simulations for the same drawbead geometry and material properties provides sufficient evidence for the reliability of the 2D plane strain drawbead model in predicting the D.B.R.F. and the plastic thickness strain [7].

3. EQUIVALENT DRAWBEAD MODEL

The equivalent drawbead model replaces the real drawbead geometry to avoid a drastic increase in CPU-time for deep drawing simulations. Besides the equivalent drawbead can be a flexible design tool; the effect of varying the position of the drawbead on the material flow can be studied very easily without the necessity to adapt the CAD-drawings for a variation in the position of the real drawbead.

In this equivalent drawbead model the real drawbead is replaced by an artificial line on the tool surface, see Figure 3. A discrete material element passing this line will experience a history dependent D.B.R.F. and thickness strain, whilst the lift force is to be subtracted simultaneously from the total blankholder force.

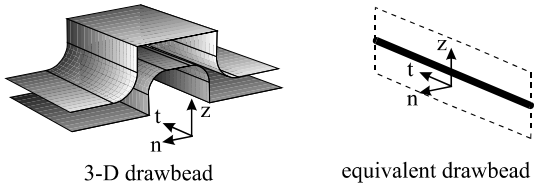

Figure 3. Schematic of a real drawbead and its equivalent representation

In the drawbead, the material flow in the normal direction ‘n’ only causes the D.B.R.F. and plastic thickness strain whereas the tangential component ‘t’ does not contribute to those, see Figure 3 [8]. This supports the approach to separate the total material flow in a normal and tangential component. Consequently, only the de normal component of the material flow is of interest for the equivalent drawbead model.

The implementation of the numerical algorithms describing the drawbead characteristics in the equivalent drawbead model will be presented in the next sub sections.

3.1 *Implementation of the lift force*

A drawbead lift force appears when material is pulled through the drawbead. The direction of the lift force is opposite to the direction of the blankholder force, causing a rise of the entire blankholder. Hence, the drawbead lift force is not a local phenomenon but will affect the total deep drawing process. The lift force is therefore subtracted from the total blankholder force during the deep drawing simulation.

3.2 *Implementation of the drawbead restraining force*

The drawbead restraining force appears as an additional force in the set of the finite element equations:

$$\underline{K} \cdot \Delta \underline{u} = \Delta \underline{f} + \Delta \underline{f}_{dbrf} \qquad \textbf{(1)}$$

where $\underline{K}$ is the stiffness matrix and $\Delta \underline{u}$ is the incremental displacement vector. The vectors on the right hand side, $\Delta \underline{f}$ and $\Delta \underline{f}_{\mathrm{dbrf}}$, denote the incremental

force vector and the additional incremental drawbead restraining force vector, respectively.

3.3 *Implementation of the plastic thickness strain*

Two numerical algorithms are implemented to add the plastic thickness strain in the equivalent drawbead model. One is based on a stress estimation [8] and one is based on a penalty constraint method. Since from [7] can be concluded that the last algorithm is preferred, only this algorithm is presented in this paper.

An extra stiffness term $\underline{K}^c{}_{db}$ and an extra incremental force vector $\Delta\underline{f}^c{}_{db}$ are added to the finite element equations to take account for the plastic thickness strain:

$$\left(\underline{K}+\underline{K}^c_{db}\right)\cdot\Delta\underline{u}=\Delta\underline{f}+\Delta\underline{f}^c_{db} \qquad \textbf{(2)}$$

The drawbead stiffness matrix $\underline{K}^c{}_{db}$ and the incremental drawbead force vector $\Delta\underline{f}^c{}_{db}$ will be derived using a constraint method.

As an illustration, the constraint equations will be derived for the element depicted in Figure 4. The nodes and the element sides are numbered arbitrarily. The element side lengths projected on the normal of the drawbead line are represented by l_i.

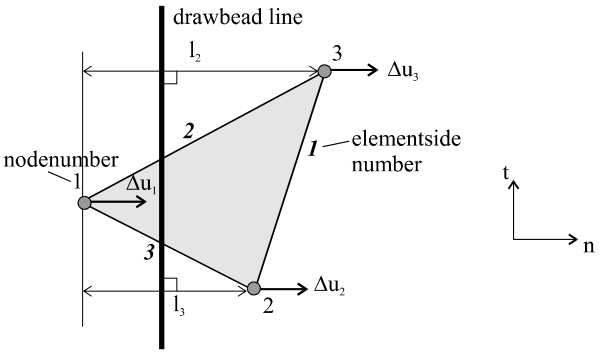

Figure 4. Node and element side numbering

A set of constraint equations can be defined for this element:

$$\begin{bmatrix}-1 & 1 & 0\\ -1 & 0 & 1\end{bmatrix}\cdot\begin{Bmatrix}\Delta u_1\\ \Delta u_2\\ \Delta u_3\end{Bmatrix}=\begin{Bmatrix}\Delta l_3\\ \Delta l_2\end{Bmatrix} \qquad \textbf{(3)}$$

where:

$$\Delta l_i = \frac{\Delta\varepsilon_{pr\_thick}\cdot l_i^{init}}{m} \qquad \textbf{(4)}$$

with $\Delta\varepsilon_{\mathrm{pr\_thick}}$ the prescribed drawbead plastic thickness strain and l_i^{init} the perpendicular element side length in the first iteration. The variable m represents the number of steps required for the entire element to pass the drawbead line.

Applying the least squares method to equation (3) and multiplying it with a penalty factor k yields:

$$k\cdot\begin{bmatrix}2 & -1 & -1\\ -1 & 1 & 0\\ -1 & 0 & 1\end{bmatrix}\cdot\begin{Bmatrix}\Delta u_1\\ \Delta u_2\\ \Delta u_3\end{Bmatrix}=k\cdot\begin{Bmatrix}-\Delta l_3-\Delta l_2\\ \Delta l_3\\ \Delta l_2\end{Bmatrix}\Rightarrow \qquad \textbf{(5)}$$

$$\underline{K}^c_{db}\cdot\Delta\underline{u}=\Delta\underline{f}^c_{db}$$

The left hand side of this formulation represents the drawbead stiffness matrix $\underline{K}^c{}_{db}$. The penalty factor is necessary to create a drawbead stiffness matrix in which the components are of the same magnitude as the components in the element stiffness matrix.

For the incremental drawbead force vector $\Delta\underline{f}^c{}_{db}$ a distinction is made between the first and the following iterations:

1^{th} *iteration:*

$$\left[\underline{K}+\underline{K}^c_{db}\right]\{\Delta\underline{u}\}=\left\{\Delta\underline{f}+\Delta\underline{f}^c_{db}\right\} \qquad \textbf{(6)}$$

n^{th} *iteration:*

$$\left[\underline{K}+\underline{K}^c_{db}\right]\{\Delta\Delta u\}=\left\{\Delta\underline{f}+\Delta\underline{f}^c_{db}-\underline{r}-\underline{r}^c_{db}\right\}$$

with $\underline{r}$ and $\underline{r}^c{}_{db}$ the reaction force vectors. For the first iteration $\Delta\underline{f}^c{}_{db}$ can be written as the right hand side vector of equation (5).

For the following iterations $\Delta\underline{f}^c{}_{db}$-$\underline{r}^c{}_{db}$ is written as:

$$\Delta\underline{f}^c_{db}-\underline{r}^c_{db}=k\cdot\begin{Bmatrix}-\Delta\Delta l_3-\Delta\Delta l_2\\ \Delta\Delta l_3\\ \Delta\Delta l_2\end{Bmatrix} \qquad \textbf{(7)}$$

with:

$$\Delta\Delta l_i=\Delta l_i-\Delta l_i^{iter}=\Delta l_i-(l_i^{iter}-l_i^{init}) \qquad \textbf{(8)}$$

where l_i^{iter} is the perpendicular element side length in the current iteration.

Adding the expressions for the stiffness matrix and force vector to the finite element equations completes the implementation of the drawbead thickness strain in the equivalent drawbead model.

4. APPLICATIONS

The equivalent drawbead model as described in section 3 is applied in deep drawing simulations of a rectangular product using two different drawbead geometry's. Experiments of these products are performed for verification of the equivalent drawbead model.

The dimensions of the two different drawbeads are listed in Table 1, where the geometry parameters are illustrated in Figure 5.

Geometry [mm]	drawbead 1	drawbead 2
R1, R3	3	3
R2	5	5
H	**8**	**5**
B1	13.6	13.6
B2	10	10
blank thickness	0.7	0.7
clearance	0.7	0.7

Table 1. Drawbead dimensions

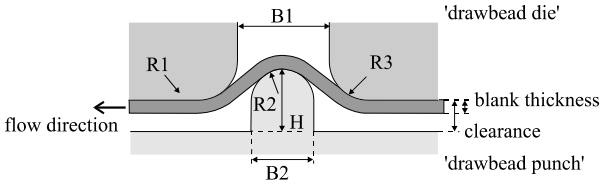

Figure 5. Drawbead geometry

The 2D plane strain drawbead model, as described in section 2, is used to determine the D.B.R.F., the lift force and the plastic thickness strain of the two different drawbeads. The results obtained with the plane strain model are given in Figure 6 and will serve as input for the equivalent drawbead model.

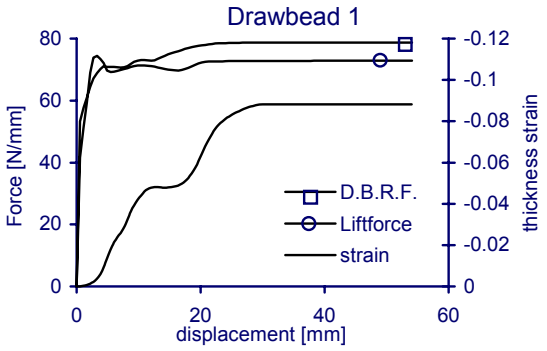

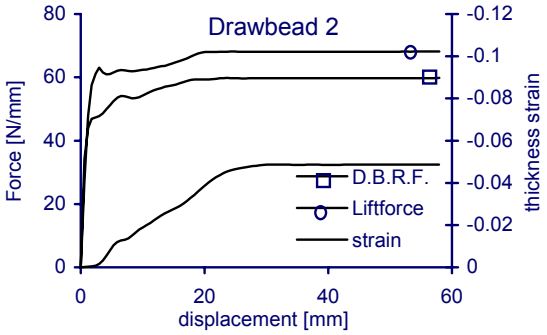

Figure 6. D.B.R.F., lift force and plastic thickness strain for both drawbeads

The tool geometry for the rectangular product is given in Figure 7. The dimensions of the tools and the blank are listed in Table 2. Drawbeads with a length of 200 [mm] are placed in the die-blank holder region, both at an distance of 126.8 [mm] in the positive and negative y-direction.

Tool description	***dimension [mm]***
punch length	400
punch width	200
radius punch shoulder	20
radius punch corner	20
die length	403.6
die width	203.6
radius die shoulder	10
radius die corner	20
product depth	100
Blank description	***dimension [mm]***
blank length	600
blank width	470
blank thickness	0.7

Table 2. Tool and blank dimensions

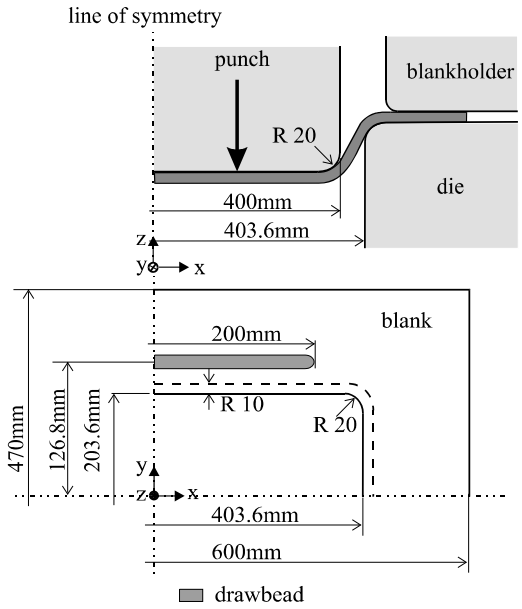

Figure 7. Tool geometry of the rectangular product

The blank is meshed with 4160 three node triangular plate elements based on Mindlin theory with 5 integration points over the height. Contact between the sheet and the tools is described with contact elements [6], in which a friction coefficient of 0.16 is assumed.

A set of simulations is performed for each of the two drawbead geometry's to test the equivalent drawbead. Initially, the material behavior in these simulations is assumed rigid plastic. A set of simulations consists of a simulation without drawbeads, a simulation in which only the D.B.R.F. is applied in the equivalent drawbead model, a simulation in which both the D.B.R.F. and the plastic thickness strain are applied and one in which the lift force is applied as well.

The draw in obtained by the deep drawing simulations of the rectangular product after 100 [mm] drawing are given in Figure 8 and 9 for the simulations including drawbeads. The simulated draw in, including the equivalent drawbead in which the D.B.R.F. and the plastic thickness strain are prescribed do hardly differ from the simulated draw in when also the lift force is prescribed. Therefore the results of one of these simulations are omitted in both figures. The experimentally determined draw in for both rectangular products are also given in these figures. The discussion of the obtained results will be focused on the draw in at the drawbead side of the rectangular product.

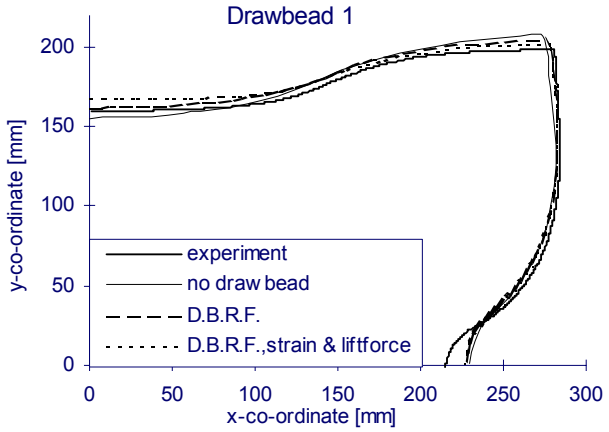

Figure 8. Flange shapes, obtained by using drawbead 1, assuming a rigid plastic material behavior

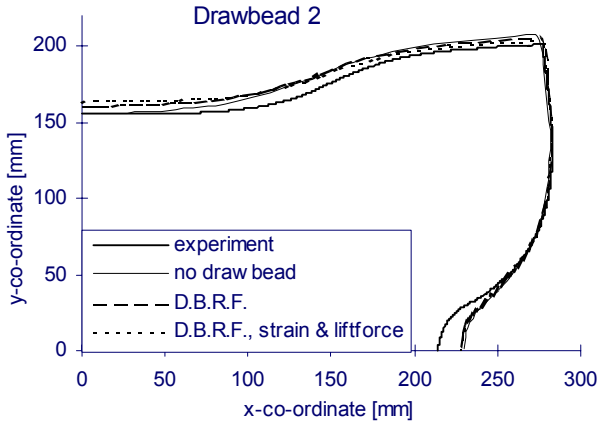

Figure 9. Flange shapes, obtained by using drawbead 2, assuming a rigid plastic material behavior

It can be concluded that the experimentally determined draw in of the rectangular product, including the different drawbeads, does not compare to the simulated draw in without using drawbeads.

As expected, the simulated draw in, including the equivalent drawbead in which only the D.B.R.F. of the different drawbeads is prescribed, shows less draw in than the simulations without drawbeads. For these simulations yields that in contrast to the simulation without drawbeads, the draw in compares less to the experimentally determined draw in.

The draw in of the product flange for both simulations with different drawbead geometry's is significantly less when the D.B.R.F., the plastic thickness strain and the lift force are prescribed in the equivalent drawbead model. For these simulations yields that the draw in compares much less to the experimentally determined draw in.

Facing the above simulation results, one can conclude that the draw in is highly underestimated

when the equivalent drawbead model is applied in the deep drawing simulations of the rectangular product. However this underestimation must not be attributed to the applied equivalent drawbead model but to the applied material model, i.e. the rigid plastic material model. The denominator of the rigid plastic material model consists of the equivalent plastic strain. Problems arise when no plastic strain occurs in some parts of a product during the deep drawing simulation. To avoid this problem, a small amount of fictive plastic strain is assumed when no plastic strain occurs. This yields for the rectangular product that plastic strain is generated in the bottom of the product and in some parts of the flange which influence the draw in of the flange negatively.

To get around this problem also a rectangular product simulation, including the equivalent drawbead model with a prescribed D.B.R.F., plastic thickness strain and lift force, is performed using an elastic plastic material model. The main advantage of the elastic plastic material description is its accuracy; the main drawback of using this description is a considerable increase in CPU-time. The results of these simulations are given in Figure 10 and Figure 11.

It can be concluded that the draw in of both simulations, including different drawbeads, compares very well with the experimentally determined draw in when the elastic plastic material model is used. Consequently, the underestimation of the draw in of the first set of simulation is indeed caused by applying the rigid plastic material model.

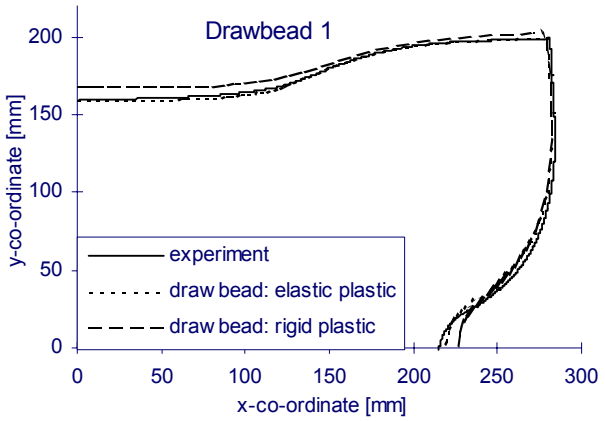

Figure 10. Flange shapes, obtained by using drawbead 1, determined with different material models

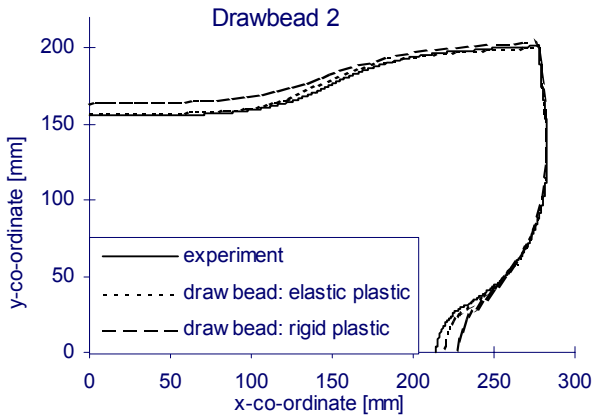

Figure 11. Flange shapes, obtained by using drawbead 2, determined with different material models

5. CONCLUDING REMARKS

- An equivalent drawbead model has been developed to avoid large computer time. The drawbead restraining force, plastic thickness strain and lift force, obtained by a 2D drawbead model serve as input for this equivalent drawbead model.
- The equivalent drawbead restrains the material flow significantly. The simulation results compare very well with the experimental results.
- The elastic plastic material model is preferred above the rigid plastic material model, since the latter underestimates the draw in of the product flange.
- The incorporation of the lift force in the equivalent drawbead has no significant effect on the simulation results.

As an overall conclusion it is stated that the equivalent drawbead model which accounts for the drawbead restraining force, the plastic thickness strain and the lift force is a powerful tool to replace the real drawbead geometry in deep drawing simulations.

6. REFERENCES

[1] Wouters P., G. Montfort, J. Defourny, 1994, *Numerical simulation and experimental evaluation of the modifications of material properties in a drawbead*, Recent developments in sheet metal forming technology, M.J.M. Barata Marques (ed.), Lisbon, p. 389-401

[2] Carleer B.D., P.T. Vreede, M.F.M. Louwes, J. Huétink, 1994, *Modeling Drawbeads with Finite Elements and Verification*, Journal of material processing technology, vol. 45/1-4, p. 63-69

[3] Kawka M., N. Wang, A. Makinouchi, 1994, *Improving drawbeads and friction models in simulations of industrial sheet metal forming processes*, Metal forming simulation in industry, B. Kröplin and E. Luckey (eds.)

[4] Taylor L.M., J. Cao, A.P. Karafillis, M.C. Boyce, 1993, *Numerical methods in sheet metal forming*, Numerical simulations of 3-D sheet metal forming processes, Makinouchi et al. (eds.)

[5] Huétink J., 1986, *On the Simulation of Thermo-mechanical Forming Processes*, Ph. D. thesis, University of Twente, Enschede, The Netherlands

[6] Huétink J., P.T. Vreede, J. van der Lugt, 1989, *The simulation of contact problems in forming processes with a mixed euler-lagrangian FE method*, Numerical methods in Industrial Forming Processes, E.G. Thompson et al. (eds.), Colorado, p. 549-554

[7] Meinders T, B.D. Carleer, H.J.M.Geijselaers, J. Huétink, 1998, *The Implementation of an Equivalent Drawbead Model in a Finite Element Code for Sheet Metal Forming*, International Journal of Materials Processing Technology, to be published

[8] Carleer B.D., T. Meinders, J. Huétink, 1996, *Equivalent drawbead model in finite element simulations*, Numerical Simulations of 3-D Sheet Metal Forming Processes, J.K. Lee et al. (eds.), Dearborn, p. 25-31